chemistry proceedings

MDPI

Proceedings

Comparative investigation of (10%Co+0.5%Pd)/TiO_2(Al_2O_3) catalysts in CO hydrogenation at low and high pressure †

Maya Shopska[1,*], Alfonso Caballero[2], Silviya Todorova[1], Katerina Aleksieva[1], Krassimir Tenchev[1], Hristo Kolev[1], Martin Fabian[3], Georgi Kadinov[1]

[1] Institute of Catalysis, Bulgarian Academy of Sciences, Sofia, Bulgaria; shopska@ic.bas.bg
[2] Inorganic Chemistry Department, Materials Science Institute (CSIC-US), Seville, Spain
[3] Institute of Geotechnics, Slovak Academy of Sciences, Kosice, Slovakia; fabianm@saske.sk
* Correspondence: shopska@ic.bas.bg; Tel.: 00359-2-979-39-18
† Presented at the 2nd International Electronic Conference on Catalysis Sciences—A Celebration of Catalysts 10th Anniversary (ECCS), online, 15-30 October 2021.

Abstract: Surface properties of prereduced (Co+Pd)/Al_2O_3 and (Co+Pd)/TiO_2 catalysts were studied. Metal dispersion was 1-3%. CoPdA demonstrated high temperature H_2 desorption and firmly held CO and carbonate species on the surface. SMSI operated on CoPdT even after contact with H_2O and air. Metal surface reconstruction and increased formation of CH_2 groups occurred during catalysis. At low pressure, CoPdT was more active whereas CoPdA had higher CH_4 selectivity. At high pressure, catalysis on CoPdA revealed dependence on T_{red}, synthesis of C_{2+} hydrocarbons, decreased CO_2 production, and higher CH_4/CO_2 ratio. CO conversion decreased with time due to difficulties in surface diffusion of reagents/intermediates/products and metal particle agglomeration.

Keywords: CO hydrogenation; cobalt-palladium catalysts; DRIFTS; low and high pressure

Citation: Shopska, M.; Caballero, A.; Todorova, S.; Aleksieva, K.; Tenchev, K.; Kolev, H.; Fabian, M.; Kadinov, G. Comparative investigation of (10%Co+0.5%Pd)/TiO_2(Al_2O_3) catalysts in CO hydrogenation at low and high pressure. *Chem. Proc.* **2021**, *3*, x. https://doi.org/10.3390/xxxxx

Published: date

1. Introduction

CO hydrogenation in synthesis gas is an environmentally friendly process, which is alternative to oil refinement [1]. Obtained products are of low or without content of nitrogen and sulphur [1,2]. The main products of the CO hydrogenation process are CH_4, CO_2, and light and heavy hydrocarbons. CH_4 and CO_2 are considered unwanted products [3,4].

Co-Pd catalysts are active in the process of CO hydrogenation [5-8]. Many factors affect their activity and selectivity [1,2,9-11]. Product distribution is influenced directly by some process parameters but others affect it indirectly through their effect on the conversion [10]. The CO hydrogenation reaction is thermodynamically favoured by increasing pressure. Since the reaction mechanism is very complex involving separate hydrogenation and polymerization routes [12], investigations at low and high pressure have been carried out to get detailed information about the reasons and ways of product distribution change. Generally, the effect of increased pressure results in enhanced CO conversion, a decrease in light hydrocarbon synthesis, and an increase of C_{5+} compound quota [2,6,9-18]. Comparative analyses at different pressures in the interval of 0.33–40 atm have been done [2,6,9,10,12-18]. A 10 atm pressure has been accepted as an optimum as result of investigations on combined influence of process parameters as pressure, temperature, H_2/CO ratio, flow rate, and conversion [12,14].

The present study discusses surface properties of alumina- and titania-supported (10%Co+0.5%Pd) catalysts and selectivity in CO hydrogenation at low and high pressure. The aim is a better understanding the specific role of the support.

2. Materials and Methods

Bimetallic catalysts with 10%Co and 0.5%Pd were prepared by deposition of metal nitrate salts from aqueous solution on non-porous TiO_2 and Al_2O_3 supports. The precursors were reduced in H_2 flow applying two modes: (i) for studies at P = 1 atm - heating at 100 and 200 °C for 1 h, and 2 h at 300 °C; (ii) for studies at P = 10 atm - heating at 260 or 400 °C for 15 h. Catalytic activity measurements were carried out at P = 1 atm and T_{reac} = 150−365 °C or P = 10 atm and 260 °C. Samples of both groups of catalysts were studied by a number of methods. Chemisorption of H_2 (at 100 °C) and CO (at 25 °C) was measured by volumetric method [19-21]. Irreversibly adsorbed CO was determined as a difference between total and reversible adsorption [22]. Particle size distribution was derived by photon cross-correlation spectroscopy (PCCS). Electron paramagnetic resonance (EPR) spectra were recorded at 25 °C in X-band. X-ray photoelectron spectra (XPS) were recorded using AlKα X-ray source. The spectra were processed according to Refs. 23 and 24. Temperature-programmed desorption (TPD) of H_2 (T_{ads}=100 °C) and CO (T_{ads} = 25 and 200 °C) was studied by differential scanning calorimeter. CO hydrogenation at 1 atm was studied *in situ* by diffuse-reflectance infrared spectroscopy (DRIFTS) in a high temperature vacuum chamber. PCCS, EPR, XPS, TPD, and DRIFTS measurements were made with catalyst samples after a CO hydrogenation test at 1 atm.

3. Results and Discussion

Two main reactions are running in our investigations at the chosen reaction conditions: (i) $CO + 3H_2 = CH_4 + H_2O$; and (ii) $CO + H_2O = CO_2 + H_2$ [25]. T_{red} and T_{reac} effect on the catalytic behaviour of the synthesized materials was examined at 1 atm in the temperature intervals 300–450 °C and 150–375 °C, respectively. A T_{red} over 300 °C led to a decrease in CO conversion and CH_4 and CO_2 yields. A definitely sharp decrease was found in the case of Al_2O_3-supported system. The observed dependences were due to metal particle agglomeration. The increase of T_{reac} resulted in an increase in CO conversion and CH_4 and CO_2 yields [6] and a decrease in the CH_4/CO_2 selectivity ratio. Values within 2–19 of the CH_4/CO_2 ratio were registered on TiO_2-supported samples in the interval T_{reac} = 285–335 °C and 3–24 for Al_2O_3-supported samples in the range 315–365 °C. These results showed that water gas-shift reaction (WGSR) was favoured to a significant extent by the temperature. (Co+Pd)/TiO_2 samples were more active and the highest activity exhibited one reduced at 300 °C (CoPdT). (Co+Pd)/Al_2O_3 samples had lower activity but demonstrated higher selectivity to CH_4 if particularly reduced at 400 °C (CoPdA).

The properties of two samples were compared, namely the most active CoPdT one reduced at 300 °C and the most selective CoPdA entity reduced at 400 °C. At the initial stage of the catalytic test H/CO ratio values of 2.9 and 2.8, respectively, were determined. Metal dispersion was calculated based on H_2 chemisorption and it was estimated to be very low as 3.61 and 1% for CoPdT and CoPdA, respectively. The data showed presence of large metal particles and a very small part of the supported metal was accessible to contact with reagents. The reasons can be related to low BET area of the titania and due to processes during decomposition of the cobalt nitrate in reductive medium followed by metal particle agglomeration facilitated by the subsequent reduction at 400 °C. In the case of CoPdA, the surface Pd atoms are highly diluted in the bimetallic particles.

In order to reveal why titania-supported catalysts were more active and those on alumina produced more CH_4, samples of both of them were studied after the catalytic tests. We considered that samples selected after catalysis would manifest surface properties that do not change or change insignificantly during subsequent studies.

A different number of peaks corresponding to particle hydrodynamic radii and representing particle size distribution in both materials characterized correlation functions obtained by PCCS. Values of the hydrodynamic radii showed that 100% of the CoPdT catalyst particles were of 40–120-nm size. For CoPdA catalyst, the result was in-

dicative about bimodal particle size distribution of 90–102 nm (58%) and 7.5–10 μm (42%). Thus, in both cases the catalyst particles were found as agglomerates.

EPR registered spectra with *g* factor of 2.2551±0.005, which was representative of tetrahedrally coordinated Co^{2+} ions [26]. Concerning their amount, it was found that CoPdT > CoPdA is valid. Perhaps, pretreatment mode and Al_2O_3 support gave rise to large amount of cobalt in diamagnetic state (Co, CoPd alloy particles and/or Co^{3+}) after reduction at 400 °C. XPS revealed also Co^{3+}, metallic Pd, and Pd^{2+}. Most probably ion presence was due to the *ex-situ* measurements, where oxygen adsorption and oxidation of the particle surface layer proceeded without penetration into the bulk while exposing to air [27,28], and/or owing to presence of unreduced phases. (Co+Pd)/support ratio of CoPdA catalyst was lower than that for CoPdT. This peculiarity was attributed to lower TiO_2 surface area, which presumed that all the metal was on the carrier grains but not in the bulk. EPR and XPS data could be assigned to higher extent of metal particle agglomeration and alloying in the CoPdA sample. On the surface of this sample, smaller amounts of carbon were registered. Deconvolution of the C1s peaks revealed that about 20% and 50% carbon with CoPdT and CoPdA, respectively, at the surface was in the form of carbonates indicating that alumina exposed stronger adsorption sites [29]. Deconvolution of the O1s spectra of CoPdT showed a composition of three sub-peaks [30] and Ti/O>0.5, which is below the stoichiometry and presupposes oxygen deficit (TiO_{2-x}). Thus, strong metal-support interaction (SMSI) has been invoked to occur during sample reduction that is preserved after catalytic runs and exposition to air.

In situ DRIFTS studies of CO hydrogenation were performed at T_{reac} = 50–250 °C. Registered bands, band maxima, and shoulders of the adsorbed species were ascribed as follows: 1767 cm^{-1} – CO multiple (bridge) bonded on Co^0; 1864 cm^{-1} – CO multiple bonded on Pd^0; 1934-90 cm^{-1} – CO bridge bonded on Pd^0 and/or linear bonded on Co^0; 2000-36 cm^{-1} – CO linear bonded on Co^0; 2040-60 cm^{-1} – CO linear bonded on $Co^{\delta+}$; 2050/60 cm^{-1} – hydrocarbonyl (H-Co-CO); and 2073-100 cm^{-1} – CO linear bonded on Pd^0 [31–35]. Registration of many bands due to one type of adsorbed CO species was assigned to existence of various sites on the metal particles with differences in nature, coordination of atoms, electronic state, and bond energy with adsorbates. Comparative analysis of the spectra during reaction showed modification of CO adsorption forms/sites with temperature change [15]. The spectral changes indicated: (i) facile CO interaction with hydrogen even at room temperature, which concerned preferably linear species; (ii) formation of new sites on CoPdT due to SMSI destruction/reduction because of synthesized H_2O reaction product [37] and because of partial oxidation of surface Co atoms by water molecules and/or reduction of residual oxide phases with formation of new adsorption centres in close contact with the support (CoPdT, CoPdA) [38,39]; and (iii) cobalt hydrocarbonyl species could contribute to some band broadening and intensity increase. When the T_{reac} was around 250 °C the bands in the CoPdT spectra decreased significantly in intensity to (almost) complete disappearance, particularly those of bridge bonded CO on Pd, thus displaying acceleration of the hydrogenation process [34] as a result of predominant dissociative adsorption of both CO and H_2 favouring formation of CH_x intermediates and CH_4 [5]. The spectra of CoPdA demonstrated significant stability of the CO adsorption on the surface *via* irreversibly adsorbed CO that is considered a precondition which further favours the hydrogenation process to methane [34,38].

Bands characteristic of hydrocarbon species were distinguished by vibrations of a CH_3 group at 1370-93, 1420-52, and 2957 cm^{-1}, a CH_2 group at 1461, 2851, and 2926 cm^{-1}, and a CH group at 1356 cm^{-1} (Fig. 4, a, b) [40,41]. With all bands, an increase of intensity was registered at $T_{reac} \geq 175$ °C for CoPdA and 150 °C for CoPdT samples. This mostly concerned the band of CH_2 groups at 2926 cm^{-1}. With CoPdT the I_{CH2}/I_{CH3} intensity ratio was 1.2–2 in the range 175–250 °C, which showed availability of sites for steady adsorption of CH_x intermediates [42,43]. Synthesized CH_4 (1303-05, 3013-16, 3099 cm^{-1}) [40,41] became perceptible at 200 and 225 °C in the spectra of CoPdT and CoPdA, respectively. Band intensities increased with T_{reac} much more with CoPdT sample in the range 225–250

°C where a 3.7-fold increase of the 3015-cm^{-1} band intensity was detected. This particularity shows that both catalysts have potential to produce higher hydrocarbons than CH_4 even at 1 atm.

(**a**) (**b**)

Figure 1. *In situ* DRIFTS spectra recorded at different temperatures during CO hydrogenation at 1 atm in presence of: (**a**) CoPdA sample; (**b**) CoPdT sample.

Bidentate (1245-68, 1566-80, 1616-18, 1640 cm^{-1}) and monodentate (1320-75, 1472, 1521-22 cm^{-1}) carbonate and formate species (1341-90, 1566-80, 1616-18 cm^{-1}) were registered on the surface of catalysts [41]. Bidentate carbonates are classified as weakly held carbonates [44] whereas desorption of formate and monodentate carbonate species takes place at higher temperatures. It can be supposed that a release of small CO_2 amounts registered with CoPdA at $T_{reac} \geq 125$ °C was due to desorption of bidentate carbonates. Thus, the results suppose existence of sites for strong adsorption of formate and carbonate species on the surface. CO_2 formation was suppressed and the catalyst gets more selective to CH_4. In the case of CoPdT the increase of T_{reac} over 150 °C facilitated the transformation of carbonate(-like) intermediate species to increase the amount of CO_2 in the gaseous phase. The catalyst manifested high activity but poor selectivity.

TPD studies showed two regions of desorption of H_2 and CO. From CoPdT sample the main amount of H_2 was desorbed at low temperatures while the situation was opposite with CoPdA. High temperature desorption of H_2 (T>360 °C) from CoPdA displayed presence of low reactive and low mobile adsorption form, which could not participate in the formation of formates and CH_4. The presence of such H_2 species can cause diminished contact of the CO with catalytically active sites, a lower number of adsorbed CO species, and increased H/CO ratio on sites generating CH_4 formation. On comparing CO species adsorbed at 25 °C and at 200 °C by TPD we observed that with CoPdT the amount of CO species desorbed at a low temperature (below ~200 °C, two types) increased with T_{ads} at the expense of those desorbed at a high temperature. Considering CoPdA the CO species desorbing at a low temperature changed only their share upon T_{ads} increase. High temperature species represented a significant part of the adsorbed CO on CoPdT at both used T_{ads}. Based on DRIFTS results, the CO desorbed at a low temperature occurs from linear and bridge bonded species whereas CO desorbed at a high temperature originates from carbonate(-like) species. Depending on T_{ads} and support, the linear CO species prevailed over the bridge forms to a different extent. All desorption peaks independent of adsorbed gas and T_{ads} fall into common temperature intervals that supposes surface species of close bonding energies and a similar structure of adsorption sites. This facilitates interaction between the species to form hydrocarbon(s) and CO_2, the latter being result of carbonate(-like) intermediate decomposition. Comparative analyses of CO_{25C}-TPD and CO_{200C}-TPD together with DRIFTS data supposed facilitated partial destruction of carbonate species, most probably those of bidentate type. Since desorption from CoPdA catalyst in the high temperature region was negligible compared to that from CoPdT, it could be assumed that the surface possesses a peculiar set of homogeneity of intermediates that contributes to a higher selectivity of the CoPdA catalyst.

Catalytic tests at 10 atm showed that the CO conversion and selectivity depended on T_{red} (Fig. 2). Methane was still the main hydrocarbon product and the CH_4/CO_2 selectivity

ratio was CoPdA > CoPdT, taking into account that the CO_2 amount produced by the CoPdT catalyst was 1.5-1.6 times higher. The CO conversion over CoPdT decreased faster with time on stream (1.4 times) after both T_{red} (260 and 400 °C), in contrast to CoPdA, which was obviously more stable especially after reduction at 400 °C.

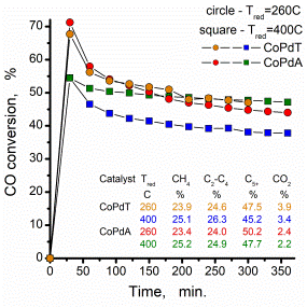

Figure 2. CO conversion at P=10 atm over the studied samples after reduction at different temperatures. Inset: Product distribution.

Selectivity was generally preserved with some changes after T_{red} = 400 °C: decreased C_{5+} and CO_2 amounts while the share of CH_4 and C_2-C_4 compounds slightly increased. The decrease in CO conversion was assigned to higher carbon deposition on the surface, difficult diffusion of reagents/intermediates/products due to synthesis of C_{5+} hydrocarbons [6,18], consumption of reagents in metal oxide reduction, and metal particle agglomeration. Reduction at 400 °C supposed higher extent of metal reduction favouring a decrease in CO_2 formation through WGSR since the number of active sites for this case as Co^{n+} decreased. CoPdT preserved higher CO_2 production most probably because of better dispersion and SMSI providing active sites. The agglomeration renders different effect on the conversion depending on carrier material. CO conversion over CoPdA was more stable due to improved resistance of the metal particles to agglomeration. In the case of CoPdT the agglomeration and SMSI (see XPS data) led to diminished CO conversion by lowering dispersion and number of active sites. By increasing metal particle size selectivity of both catalysts to different hydrocarbons is changed because the formation and homogenization of the bimetallic particle surface is facilitated. Modified properties of the surface cobalt atoms and larger particle size favoured CO dissociation over cobalt [15,36]. Together with the effect of increased pressure, the probability for polymerization and carbon chain growth is augmented. However, increased P_{H2} enriched the surface in CH_x species [1,9,11] and helped to divide bigger intermediates into smaller fragments and thus decreased chain growth to some extent in situation of slightly enhanced CO dissociation [9]. In the case of CoPdA catalyst, the increased P_{H2} could contribute to stable CO conversion avoiding deactivation of metal by oxidation during the process [15].

4. Conclusions

Co-Pd catalysts with alumina support pretreated in H_2 were more selective toward methane and produced lower CO_2 amount during CO hydrogenation at 1 atm compared to catalysts with titania. The properties were preserved in the reaction at 10 atm due to strong metal-support interaction in CoPdT, which was not reduced by contact with H_2O and air, thus determining sites for carbonate species formation and CO_2 production. CoPdT produced a lower C_{5+} amount because of stable adsorption of CH_x intermediates.

Author Contributions: Conceptualization, writing—original draft preparation, visualization, project administration, funding acquisition, M.Sh.; methodology, M.Sh., S.T., A.C. and G.K.; validation, M.Sh., S.T., A.C., H.K., M.F., K.A., K.T.; investigation, M.Sh., H.K., M.F., K.A., K.T., S.T., A.C., G.K.; resources, M.Sh., S.T., A.C.; data curation, M.Sh., S.T., A.C., H.K., M.F., K.A., K.T.; writing—review and editing, G.K.; supervision, S.T., A.C. and G.K. All authors have read and agreed to the published version of the manuscript.

Funding: This research was funded by Bulgarian National Science Fund, contract number KP-06-H29-9/2018.

Data Availability Statement: IC, BAS, Sofia, Bulgaria; ICD, MSI (CSIC-US), Seville, Spain; IG, SAS, Kosice, Slovakia.

Acknowledgments: English language editing by Assoc. Prof. Ch. Bonev is appreciated.

Conflicts of Interest: The authors declare no conflict of interest.

References

1. Zhang, Q.; Kang, J.; Wang, Y. Development of novel catalysts for Fischer–Tropsch synthesis: tuning the product selectivity. *ChemCatChem.* **2010**, *2*, 1030-1058, DOI: 10.1002/cctc.201000071
2. Riyahin, M.; Atashi, H.; Mohebbi-Kalhori, D. Optimization of reaction condition on the product selectivity of Fischer-Tropsch synthesis over a Co-SiO_2/SiC catalyst using a fixed bed reaction. *Petroleum Sci. Technol.* **2017**, *35*, 1078-1084, DOI: 10.1080/10916466.2017.1303715
3. Schmidt-Rohr, K. Why combustions are always exothermic, yielding about 418 kJ per mole of O_2. *J. Chem. Education* **2015**, *92*, 2094–2099, DOI: 10.1021/acs.jchemed.5b00333
4. Murdoch, A. Structural and compositional analysis of Co-Pd model catalyst surfaces, PhD Thesis, University of St. Andrews, 2012.
5. Davis, B. H.; Iglesia, E. Technology development for iron and cobalt Fischer-Tropsch catalysts, Final technical report DE-FC26-98FT40308, University of California at Berkeley & University of Kentucky Research Foundation, June 30, 2002.
6. Arsalanfar, M.; Mirzaei, A. A.; Bozorgzadeh, H. R.; Samimi, A. A review of Fischer–Tropsch synthesis on the cobalt based catalysts. *Phys. Chem. Res.* **2014**, *2*, 179-201, DOI: 10.22036/pcr.2014.5786
7. Rabo, J. A.; Risch, A. P.; Poutsma, M.L. Reactions of carbon monoxide and hydrogen on Co, Ni, Ru, and Pd metals. *J. Catal.* **1978**, *53*, 295-311
8. Dinse, A.; Aigner, M.; Ulbrich, M.; Johnson, G.R.; Bell, A.T. Effects of Mn promotion on the activity and selectivity of Co/SiO_2 for Fischer-Tropsch synthesis. *J. Catal.* **2012**, *288*, 104-114, DOI:10.1016/j.jcat.2012.01.008
9. Sari, A.; Zamani, Y.; Taheri, S. A. Intrinsic kinetics of Fischer-Tropsch reactions over an industrial Co-Ru/γ-Al_2O_3 catalyst in slurry phase reactor. *Fuel Proc. Technol*. **2009**, *90*, 1305-1313, DOI: 10.1016/j.fuproc.2009.06.024
10. Gibson, E. J.; Hall, C. C. The Fischer-Tropsch synthesis with cobalt catalysts: the effect of process conditions on the composition of the reaction products. *J. Appl. Chem.* **1954**, *4*, 49-61
11. Zhou, W.; Chen, J.-G.; Fang, K.-G.; Sun, Y.-H. The deactivation of Co/SiO_2 catalyst for Fischer-Tropsch synthesis at different ratios of H_2 to CO. *Fuel Proc. Thechnol*. **2006**, *87*, 609-616
12. Mirzaei, A. A.; Shirzadi, B.; Atashi, H.; Mansouri, M. Modeling and operating conditions optimization of Fischer-Tropsch synthesis in a fixed-bed reactor. *J. Ind. Eng. Chem.* **2012**, *18*, 1515-1521, DOI: 10.1016/j.jiec.2012.02.013
13. Kwack, S.-H.; Park, M.-J.; Bae, J. W.; Ha, K.-S.; Jun, K.-W. Development of a kinetic model of the Fischer-Tropsch synthesis reaction with a cobalt-based catalyst. *Reac. Kinet. Mech. Catal* . **2011**, *104*, 483-502, DOI: 10.1007/s11144-011-0369-1
14. Jalama, K. Chapter 39 - Effect of operating pressure on Fischer-Tropsch synthesis kinetics over titania-supported cobalt catalyst. In: *Transactions on engineering technologies, World Congress on Engineering and Computer Science 2015*; Ao, S.-I. , Kim, H. K., Amouzegar, M. A., Eds.; Springer, Singapore 2017; pp. 555-562, DOI: 10.1007/978-981-10-2717-8_39
15. de la Pena O'Shea, V. A.; Alvarez-Galavan, M. C.; Campos-Martin, J. M.; Fierro, J. L. G. Strong dependence on pressure of the performance of a Co/SiO_2 catalyst in Fischer-Tropsch slurry reactor synthesis. *Catal. Lett*. **2005**, *100*, 105-110, DOI: 10.1007/s10562-004-3096-7
16. Geerlings, J. J. C.; Wilson, J. H.; Kramer, G. J.; Kuipers, H. P. C. E.; Hoek, A.; Huisman, H. M. Fischer-Tropsch technology – from active site to commercial process. *Appl. Catal. A: Gen.* **1999**, *186*, 27-40
17. Yates, I. C.; Sattarfield, C. N. Hydrocarbon selectivity from cobalt Fischer-Tropsch catalysts. *Energy and Fuels* **1992**, *6*, 308-314
18. Yan, Z.; Wang, Z.; Bukur, D. B.; Goodman, D. W. Fischer-Tropsch synthesis on a model Co/SiO_2 catalyst. *J. Catal.* **2009**, *268*, 196-200, DOI: 10.1016/j.jcat.2009.09.015
19. Aben, P. C. Palladium areas in supported catalysts: Determination of palladium surface areas in supported catalysts by means of hydrogen chemisorption. *J. Catal.* **1968**, *10*, 224
20. Reuel, R. C.; Bartholomew, C. H. The stoichiometries of H_2 and CO adsorptions on cobalt: Effects of support and preparation. *J. Catal.* **1984**, *85*, 63
21. Zowtiak, J. M.; Bartholomew, C. H. The kinetics of H_2 adsorption on and desorption from cobalt and the effects of support thereon. *J. Catal.* **1983**, *83*, 107
22. Anderson, J. R. *Structure of metallic catalysts*; Mir: Moscow, Russia, 1978 (in Russian).
23. Shirley, D. A. High-resolution X-ray photoemission spectrum of the valence bands of gold. *Phys. Rev. B* **1972**, *5*, 4709-4714
24. Scofield, J. H. Hertree-Slater subshell photoionization cross-sections at 1254 and 1487 eV. *J. Electron Spectrosc. Relat. Phenom.* **1976**, *8*, 129-137, DOI: 10.1016/0368-2048(76)80015-1
25. Zheng, S.; Liu, Y.; Li, J.; Shi, B. Deuterium tracer study of pressure effect on product distribution in the cobalt-catalyzed Fischer-Tropsch synthesis. *Appl. Catal. A: Gen*. **2007**, *330*, 63-68, DOI: 10.1016/j.apcata.2007.07.010

26. Guskos, N.; Typek, J.; Maryniak, M.; Żolnierkiewicz, G.; Podsiadly, M.; Arabczyk, W.; Lendzion-Bielun, Z.; Narkiewicz, U. Effect of calcination and structural additives on the EPR spectra of nanocrystalline cobalt oxides. *Mater. Sci.-Poland* **2006**, *24*, 4
27. Popova N. M.; Babenkova L. V.; Savel'eva G. A. *Adsorption and interaction of the simplest gases with metals from VIII group*. Nauka: Alma-Ata, Kazakhstan, 1979 (in Russian).
28. Potoczna-Petru, D.; Jablonski, J. M.; Okal, J.; Krajczyk, L. Influence of oxidation-reduction treatment on the microstructure of Co/SiO_2 catalyst. *Appl. Catal. A: Gen.* **1998**, *175*, 113-120
29. Singh, B.; Patial, J.; Sharma, P.; Chandra, S.; Maity, S.; Lingaiah, N. A comparative study on basicity based on supported K-salt catalysts for isomerization of 1-methoxy-4-(2-propene-1-yl) benzene. *Indian J. Chem. Technol.* **2010**, *17*, 446-450
30. Pan, X.; Yang, M.-Q.; Fu, X.; Zhang, N.; Xu, Y.-J. Defective TiO_2 with oxygen vacancies: synthesis, properties and photocatalytic applications. *Nanoscale* **2013**, *5*, 3601-3614, DOI: 10.1039/c3nr00476g
31. Zhang, J.; Chen, J.; Ren, J.; Sun, Y. Chemical treatment of γ-Al_2O_3 and its influence on the properties of Co-based catalysts for Fischer–Tropsch synthesis. *Appl. Catal. A* **2003**, *243*, 121
32. Tsubaki, N.; Sun, S.; Fujimoto, K. Different functions of the noble metals added to cobalt catalysts for Fischer–Tropsch synthesis. *J. Catal.* **2001**, *199*, 236
33. Kadinov, G.; Bonev, Ch.; Todorova, S.; Palazov, A. IR spectroscopy study of CO adsorption and of the interaction between CO and hydrogen on alumina supported cobalt. *J. Chem. Soc. Faraday Trans.* **1998**, *94*, 3027-3031
34. Singh, J. A.; Yang, N.; Liu, X.; Tsai, C.; Stone, K. H.; Johnson, B.; Koh, A. L.; Bent, S. F. Understanding the active sites of CO hydrogenation on Pt-Co catalysts prepared using atomic layer deposition. *J. Phys. Chem. C* **2018**, *122*, 2184-2194, DOI: 10.1021/acs.jpcc.7b10541
35. Xiong, H.; Zhang, Y.; Liew, K.; Li, J. Ruthenium promotion of Co/SBA-15 catalysts with high cobalt loading for Fischer-Tropsch synthesis. *Fuel Proc. Technol.* **2009**, *90*, 237-246, DOI: 10.1016/j.fuproc.2008.08.014
36. Tuxen, A.; Carenco, S.; Chintapalli, M.; Chuang, C.-H.; Escudero, C.; Pach, E.; Jiang, P.; Borondics, F.; Beberwyck, B.; Alivisatos A. P.; Thornton, G.; Pong, W.-F.; Guo, J.; Perez, R.; Besenbacher, F.; Salmeron, M. Size-dependent dissociation of carbon monoxide on cobalt nanoparticles. *J. Am. Chem. Soc.* **2013**, **135**, 2273-2278, DOI: 10.1021/ja3105889
37. Li J., Xu L., Keogh R.A., Davis B.H. Effect of boron and ruthenium on the catalytic properties of Co/TiO2 Fischer-Tropsch catalysts. *ACS Div. Petr. Chem., Preprints* **2000**, *45*, 253 (219th National Meeting, ACS, San Francisco, CA, March 26-31, 2000)
38. Sun, X.; Sartipi, S.; Kapteijn, F.; Gascon, J. Effect of pretreatment atmosphere on the activity and selectivity of Co/*meso*HZSM-5 for Fischer–Tropsch synthesis. *New J. Chem.* **2016**, *40*, 4167-4177, DOI: 10.1039/c5nj02462e
39. Chen, T.-Y.; Su, J.; Zhang, Z.; Cao, C.; Wang, X.; Si, R.; Liu, X.; Shi, B.; Xu, J.; Han, Y.-F. Structure evolution of Co-CoO_x interface for higher alcohol synthesis from syngas over Co/CeO_2 catalysts. *ACS Catal.* **2018**, *8*, 8606-8617
40. Sanchez-Escribano, V.; Larrubio-Vargas, M. A.; Finocchio, E.; Busca, G. On the mechanisms and the selectivity determining steps in syngas conversion over supported metal catalysts: An IR study. *Appl. Catal. A: Gen.* **2007**, *316*, 68-74, DOI: 10.1016/j.apcata.2006.09.020
41. Little, L. H. *Infrared Spectra of Adsorbed Species*; Academic Press Inc.: London, New York, 1966.
42. Geerlings, J. J. C.; Zonnevylle, M. C.; de Groot, C. P. M. Studies of the Fischer-Tropsch reaction on Co(0001). *Surf. Sci.* **1991**, *241*, 302-314
43. Geerlings, J. J. C.; Zonnevylle, M. C.; de Groot, C. P. M. Structure sensitivity of the Fischer-Tropsch rection on cobalt single crystals. *Surf. Sci.* **1991**, *241*, 315-324
44. Szanyi, J.; Kwak, J. H. Dissecting the steps of CO_2 reduction: 1. The interaction of CO and CO_2 with γ-Al_2O_3: an *in situ* FTIR study. *Phys. Chem. Chem. Phys.* **2014**, *16*, 15117-15125, DOI: 10.1039/c4cp00616j